# Computational ghost imaging by means of Fourier spectrum acquisition

Author: Eric Bataller Thomas
*Facultat de Física, Universitat de Barcelona, Diagonal 645, 08028 Barcelona, Spain.**

Advisor: Dr. Artur Carnicer Gonzalez

**Abstract:** Computational ghost imaging (CGI) is a innovative technique capable of performing imaging with a single-pixel detector (SP) by illuminating the scene with an ensemble of random patterns and calculating the correlation of those patterns and the object. Therefore, it's based on a statistical model. Nevertheless, this way of carrying out an image reconstruction presents some issues regarding long data-acquisition time and a low reconstruction quality. Recently, a new computational imaging technique called Fourier ghost imaging (FGI) was proposed which can reconstruct images by acquiring their Fourier spectrum, therefore making use of a deterministic model. Simulations on both methods are performed with its corresponding analysis on the efficiency and their robustness against noise. Our work may provide a guideline for researchers to decide whether or not they use a ghost imaging technique.

## I. INTRODUCTION

Over the last two decades, ghost imaging (GI) has aroused great concern for counter-intuitive imaging mechanism due to its capability of reconstructing images with a single-pixel detector. In conventional imaging techniques, the object is recorded by spatially resolved detectors such as through a charge-coupled device (CCD) camera. However, in GI the same reconstruction can be achieved by single-pixel detector, like a photodiode (PD).

The GI enables robust imaging against noise, owing to statistical correlation processing between a known reference and an unknown object intensity field. Therefore, given the time series data obtained from the detector, the effect of turbulence or scattering media between the object and the detector planes can be widely reduced.

Ghost imaging was initially considered as a quantum effect making use of random patterns coming from spontaneous parametric down-conversion [1] or speckle patterns generated by a laser beam and a rotating ground-glass [2]. Both methods use a beam splitter, dividing in two arms the optical setup and making the one beam that interacts with the object be collected by the single-pixel detector (often called bucket detector).

Thereafter, computational ghost imaging was introduced by Shapiro in [3]. CGI combines computer generated random patterns and a spatial light modulator (SLM) to obtain the reference field. If instead of using laser light, incoherent light is used, there will be no need for free-space propagation calculation [4]. Thus, the intensity of the object plane is computationally obtained without a camera, significantly simplifying the optical setup.

Due to its potential, several applications of CGI have been studied in different fields such as 3D imaging [4], color imaging [5],phase retrieval [6], thermal light imaging [7], astronomical ghost imaging [9], optical encryption [10], X-ray ghost tomography [8] and so on. Especially, ghost imaging becomes very interesting for those who need minimally invasive imaging techniques under weak illumination (e.g. in the biomedical field to avoid photobleaching).

One of the major problems CGI faces is the fact that to be able to achieve sharp images, it requires a large number of patterns to be projected over the object, which makes it more time-consuming. To improve the performance of CGI, several algorithms have been designed in order to increase the signal-to-noise ratio (SNR) of the pictures allowing them to reconstruct better images within less pattern projections (e.g. differential ghost imaging [11], normalized ghost imaging [12], or correlation of powers of intensity [13]). Although these methods can improve the results of the GI, they still require a large number of measurements and a long computation time (for large images, it might be a few hours or more). To overcome these problems, a new approach arises: Instead of projecting random patterns taken from a nonorthogonal basis onto the object, we rather use orthogonal patterns to do so. Thus, improving the image contrast with much smaller number of patterns and making the reconstruction computation into a deterministic model (in contrast to ghost image which is designed as a statistical model). Several orthogonal basis were proposed such as Hardaman patterns [14], wavelet transform patterns [15], principal component analysis patterns [16], and the one we will analyse in this paper: Fourier sinusoidal patterns [17].

Fourier ghost imaging achieves reducing the number of measurements and the computation time by the illumination of sinusoidal patterns and the reconstruction algorithm based on the Fourier spectrum acquisition and its posterior Fourier transform. Besides constituting an orthogonal basis, FGI is good for reconstructing images in a fast way given the fact that, in general, low frequencies contain much more image information than the higher ones, making the quality of the image improve drasti-

*Electronic address: ebatalth7@alumnes.ub.edu

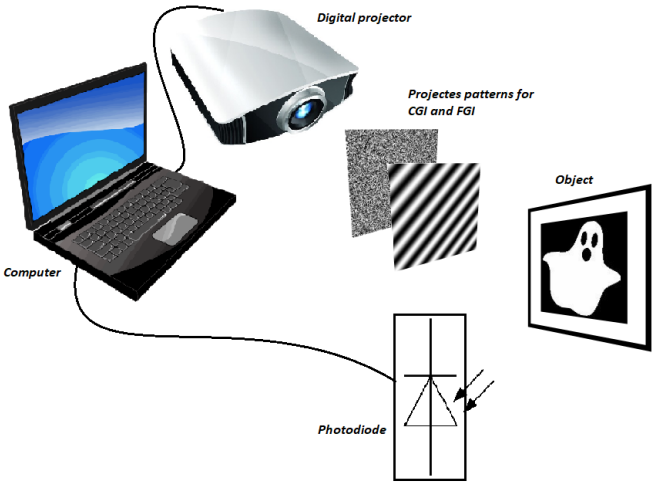


FIG. 1: Scheme of the optical setup of the ghost imaging and fourier ghost imaging technique.

cally within a few measurements on the single-pixel. We confirm the feasibility of the method and, by carrying out numerical simulations, conclude that the method outperforms the CGI method in terms of efficiency and turns out to be useful in high-SNR situations.

In Fig.(1) a simplified scheme of the optical setup is shown to perfrom CGI and FGI.

## II. PRINCIPLE OF CGI AND FGI

In this section we give a brief explanation of CGI and FGI, which have been described in detail elsewhere [3, 17]. For the sake of simplicity, we will assume that the SLM plane corresponds to the object plane. The object is illuminated by a random pattern displayed on the SLM. The scattered light is collected by a lens and focalized into the single-pixel detector. This process is repeated a large number of times while changing the patterns. The intensity measured in the SP, $I_0$, is described as:

$$D_0 = \int_{beam\ area} O(x,y) I_r(x,y)\, dxdy, \tag{1}$$

where O(x,y) is the object function (the one we want to reconstruct) and $I_r(x,y)$ is the intensity distribution of the rth pattern, $r = 1, 2, 3, ..., n$, n being the number of measurements. This can be calculated from a computational perspective as the inner product between the pattern (no matter what the basis is) and the object.

According to CGI, the object image is reconstructed by calculating the correlation between the random pattern distributions $I_r(x,y)$ and their corresponding measurements in the SP $D_0$. The retrieved image G(x,y) is described as

$$\begin{aligned} G(x,y) &= \frac{1}{n}\sum_{r=1}^{n}(D_0 - \langle D_0\rangle) I_r(x,y) \\ &= \langle D_0 I(x,y)\rangle - \langle D_0\rangle \langle I(x,y)\rangle\,, \end{aligned} \tag{2}$$

where $\langle ...\rangle$ denotes the ensemble average over the n measurements. Thus, given that $D_0$ is given by Eq.(1), G(x,y) converges to O(x,y) as n increases. The Eq.(2) reflects that the object image is estimated by the correlation value of each pattern. In FGI, we seek to acquire the Fourier spectrum first and thereafter, to retrieve the image by applying an inverse Fourier transform. Fourier spectrum is composed by a group of coefficients. Each one of those correspond to a unique sinusoidal pattern with a specific frequency and therefore, is the visualization of how the function is decomposed into a set of orthogonal sinusoidal waveforms of different frequencies. To obtain such coefficients, one can project sinusoidal patterns onto the object and measure its correlation with the single-pixel detector. Thus, knowing how strongly correlated that pattern with a specific frequency is with the object. The reconstructed the Fourier spectrum of a 2D function (the image G(x,y)), The Fourier transform F is described as:

$$\begin{aligned} \tilde{G}(u,v) &= F\{G(x,y)\} \\ &= \sum_{x=0}^{M-1}\sum_{y=0}^{N-1} G(x,y) exp\left[-j2\pi\left(\frac{ux}{M} + \frac{vy}{N}\right)\right], \end{aligned} \tag{3}$$

where u and v are the spatial frequencies, and M and N are the number of pixels the image will have on the x and y axis, respectively. The Fourier basis patterns can be obtained by applying an inverse Fourier transform $F^{-1}$to a delta function $\tilde{\delta}(u,v,\phi)$.

$$\tilde{\delta}(u,v,\phi) = \begin{cases} exp(j\phi) & u = u_0\ and\ v = v_0 \\ 0 & elsewhere \end{cases} \tag{4}$$

where $\phi$ is a parameter we put in order to choose the phase of our sinusoidal pattern so to be able to retrieve the phase information (which is the most important in an image). The sinusoidal pattern is therefore computed as:

$$I_\phi(x,y) = \frac{1}{2}\left[1 + \left|F^{-1}\left\{\tilde{\delta}(u,v,\phi)\right\}\right|\right] \tag{5}$$

For the FGI reconstruction, since Fourier coefficients $F(u,v)$ are complex-valued they need to be acquired within the projection of more than one pattern. In our case, this will be done by projecting 4 different patterns $I_0(x,y)$,$I_\pi(x,y)$, $I_{\frac{\pi}{2}}(x,y)$ and $I_{\frac{3\pi}{2}}(x,y)$ and using their respective measurements in the single-pixel detector $D_0$,$D_\pi$, $D_{\frac{\pi}{2}}$ and $D_{\frac{3\pi}{2}}$ to be able to obtain the real

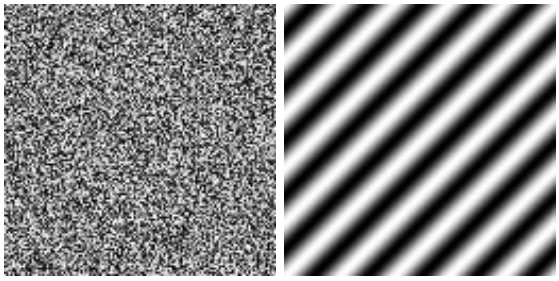

(a) CGI pattern (b) FGI pattern

FIG. 2: Typical patterns used in CGI (a) and FGI (b)

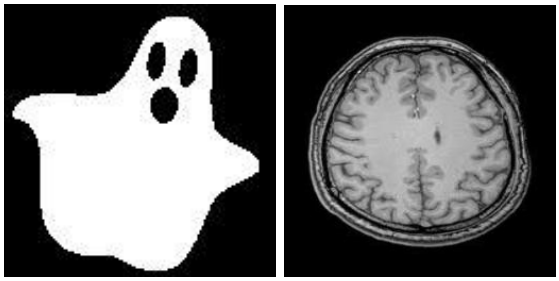

(a) Ghost (b) Brain

FIG. 3: a) 128x128-pixel binary image of a ghost. b) 256x256-pixel grayscale image of a brain.

and the imaginary part of the coefficient in the following way:

$$F(u,v) = (D_0 - D_\pi) + j(D_{\frac{\pi}{2}} - D_{\frac{3\pi}{2}}) \tag{6}$$

This data acquisition will be on going until we get to the frequency in which we want to stop (this frequency can be limited by the SLM resolution). Finally, we can obtain $G(x,y)$ matrix by computing the inverse Fourier transform of the Fourier spectrum. For this type of FGI, to fully sample a $M \times N$ pixel image it will take $4 \times M \times N$ measurements to do a complete reconstruction of the Fourier spectrum. But with the prior knowledge that the Fourier spectrum for real-value functions (like an image) is conjugated symmetric, the number of measurements boils down to $n = 2 \times M \times N$.

In Fig.(2), two typical patterns from the CGI and FGI ensemble are shown.

## III. NUMERICAL SIMULATIONS

To compare the feasibility and the quality of both methods, we carried out numerical simulations. We simulated CGI by using random patterns and FGI by using sinusoidal patterns like the one in Fig.(2b). Since sampling strategies may change the quality of the reconstructed images of FGI, we will use the circular path acquisition since it has been proved to be the best one for general purposes according to [18].The sampling strategy refers to the path along which the Fourier coefficients are to be acquired. In our case, circular path means that we retrieve the coefficients from low to high frequencies in a circular way.

Two test objects were used to see the quality of the reconstructions (see Fig.(3)). Images of a ghost and a brain were reconstructed for different numbers of samples and numerical results are shown in Fig.(4) and Fig.(5), respectively. Notice that for the FGI the percentage of spectrum acquired is given along with the number of patterns projected.

As can be seen in Fig.(4) and Fig.(5), FGI outperforms CGI not only in terms of quality in the reconstruction but also in terms of efficiency, given the fact that the image is fully retrieved with maximal quality once we have projected all the orthogonal pattern basis onto the object. For the sake of clarity, quantitative analysis has been made into the reconstructed images by calculating the structural similarity (SSIM) index to compare the quality. SSIM is defined as:

$$SSIM = \frac{(2\mu_G\mu_O + c_1)(2\sigma_{GO} + c_2)}{(\mu_G^2 + \mu_O^2 + c_1)(\sigma_G^2 + \sigma_O^2 + c_2)} \tag{7}$$

where $\mu_G$ and $\mu_O$ are the average value of $G(x,y)$ and $O(x,y)$; $\sigma_G$ and $\sigma_O$ are their variance; $\sigma_{GO}$ is the covariance between $G(x,y)$ and $O(x,y)$; $c_1 = (k_2 * L)^2$ and $c_2 = (k_2 * L)^2$ are the constant with $K_1 = 0.1$ and $K_2 = 0.03$; $L$ is the dynamic range of the grayscale values. Note that, SSIM is a comprehensive index that can reflect the contrast, brightness and structural information of the image, widely used in image processing. This index runs from 0 to 1 ( being 1 the maximal similarity and 0 the minimal).

The results obtained in the comparison can be seen in the following tables for the ghost and the brain, respectively.

Looking at the tables (I) and (II) we clearly see that FGI is much more efficient, being able to fully reconstruct the image. I addition, we see a rapid increase in the SSIM during the first projections, reaching in both cases the 0.2 within less than a 1% of spectrum acquisition. This phenomena is due to the fact that, when decomposed in their

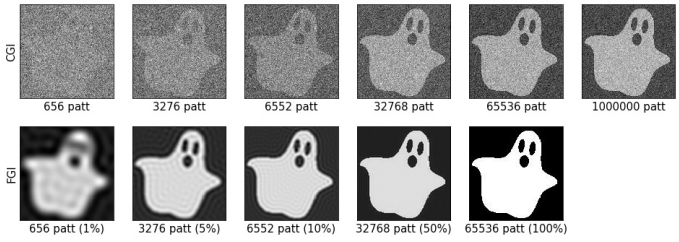


FIG. 4: Numerical results of CGI and FGI in free-noise condition for the ghost image.

| n° patterns | 656 (1%) | 3276 (5%) | 6552 (10%) | 32768 (50%) | 65536 (100%) | 1000000 |
|---|---|---|---|---|---|---|
| CGI | 0.05 | 0.09 | 0.12 | 0.19 | 0.20 | 0.26 |
| FGI | 0.29 | 0.40 | 0.45 | 0.53 | 1 | |

TABLE I: SSIM index for the different ghost images for a given number of patterns (and, in the case of FGI, also the percentage of acquisition).

| n° patterns | 2620 (1%) | 13108 (5%) | 26212 (10%) | 131072 (50%) | 262144 (100%) | 1000000 |
|---|---|---|---|---|---|---|
| CGI | 0.05 | 0.09 | 0.11 | 0.19 | 0.21 | 0.27 |
| FGI | 0.23 | 0.41 | 0.48 | 0.58 | 1 | |

TABLE II: SSIM index for the different brain images for a given number of patterns (and, in the case of FGI, also the percentage of acquisition).

frequencies, most of the images have strong low-frecuency components, meaning that their spectrum is very "energetic" at the center compared to the magnitudes of the components on the high-frequency zone. This allows FGI to be able to perform a reliable reconstruction within a few pattern projections. Thus, making it a faster method capable of taking good pictures while being in undersampling conditions.

In order to study the robustness of both methods against noise, we studied how they respond by varying the signal to noise ratio (SNR). A Gaussian distributed noise on the output of the detector is superimposed. It has been assumed here, that the incident light on the single-pixel detector was in the range of 0-1. In a similar way that Shibuya and colleagues did in [19] to study the noise robustness of Hardaman transform imaging, let us add a Gaussian noise of center value and variance $\sigma^2$ of zero and $9\times10^{-8}$, respectively. Therefore, by varying the light intensity of the signal from $1.8 \times 10^{-5}$ to $2 \times 10^{-2}$, we look at the reconstruction of the images within a SNR range from 0.03 to 33.

Fig.(6) shows the results of the reconstruction of the image, where noise was added at the output of the single-pixel detector. Two different number of samples n are used in the reconstruction of CGI: $n = 65536$ and $n = 1000000$. For the FGI reconstruction only $n = 65536$ is shown. If we take a look at the results,we will see that the noise is progressively suppress by increasing n in the CGI. The visibility of the reconstructions by FGI is still higher than the ones performed by CGI under the same number of projections for high-SNR conditions. Nevertheless, for low-SNR conditions, the visibility is practically the same. Thus, both methods are affected by noise in a similar way, but the fact that FGI can retrieve a better image within the same number of projections, gives it an advantage to perform better. On the other hand, if the data-acquisition time is not a problem, and our main target is to reduce noise, an interesting solution given its simplicity could be using CGI for a large number of measurements.

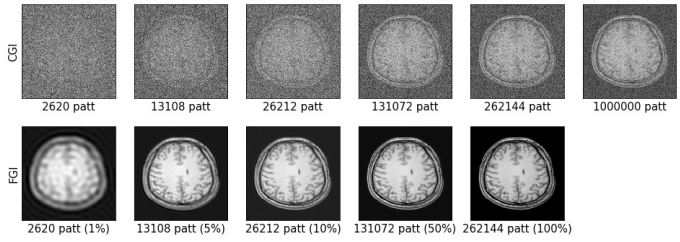


FIG. 5: Numerical results of CGI and FGI in free-noise condition for the brain image.

## IV. CONCLUSIONS

In this study we performed some numerical simulations regarding two unconventional imaging techniques: computational ghost imaging (CGI) and Fourier ghost imaging (FGI). Thus, confirming their feasibility. The given results have shown that FGI outperforms CGI in terms of efficiency and quality. By making use of the Fourier spectrum properties such as its symmetry and its energy concentration in the low-frequency zone, and given the fact that we are dealing with a deterministic model due to the orthogonal basis patterns that we are projecting, this method obtains a great advantage over CGI and gives rise to a very interesting solution to the original problems of CGI regarding long data-acquisition time and a low reconstruction quality.

A comparative study was carried out between computational ghost imaging (CGI) and Fourier ghost imaging (FGI) under various SNR condition, confirming that the recent method FGI is more useful than CGI for a fixed total number of illuminations n under high-SNR conditions. Nevertheless, CGI might be an interesting solution to enable the visibility by simply increasing the number of measurements n (and therefore the acquisition time).

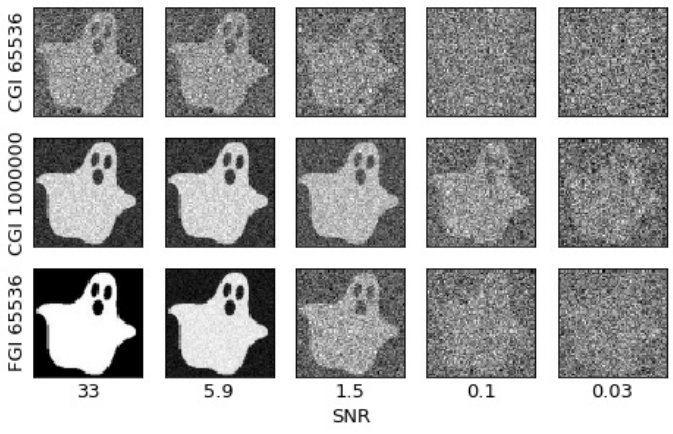


FIG. 6: Numerical results of the reconstruction of the ghost image by CGI for $n = 65536$ and $n = 1000000$ and FGI for $n = 65536$, where noise was added at the output of the single-pixel detector.

**Acknowledgments**

We would like to express our special thanks and gratitude to Dr. Arthr Carnicer for introducing me to the topic and for his valuable discussion and suggestions, as well as Dunya Harb for linguistic assistance. This work was supported by the Univeristy of Barcelona.

[1] T. B. Pittman, Y. H. Shih, D. V. Strekalov, and A. V. Sergienko."Optical imaging by means of two-photon quantum entanglement". Phys. Rev. A **52**, R3429 (1995).

[2] G. Scarcelli, V. Berardi, and Y. Shih."Can Two-Photon Correlation of Chaotic Light Be Considered as Correlation of Intensity Fluctuations?". Phys. Rev. Lett. **96**, 063602 (2006).

[3] 3. J. H. Shapiro, "Computational ghost imaging" Phys. Rev. A **78**, 061802 (2008).

[4] B. Sun, M. P. Edgar, R. Bowman, L. E. Vittert, S. Welsh, A. Bowman,and M. J. Padgett, "3D Computational Imaging with Single-Pixel Detectors" Science **340**, 844 (2013).

[5] S. S. Welsh, M. P. Edgar, P. Jonathan, B. Sun, and M. J. Padgett, "Multi-wavelength compressive computational ghost imaging," Proc. SPIE **8618**, 86180I (2013).

[6] L. Martínez-León, P. Clemente, Y. Mori, V. Climent, J. Lancis, and E. Tajahuerce, "Single-pixel digital holography with phase-encoded illumination," Opt. Express **25**, 4975–4984 (2017).

[7] X.-H. Chen, Q. Liu, K.-H. Luo, and L.-A. Wu, "Lensless ghost imaging with true thermal light," Opt. Lett. **34**, 695–697 (2009).

[8] A. M. Kingston, G. R. Myers, D. Pelliccia, I. D. Svalbe, and D. M.Paganin, "X-ray ghost tomography: denoising, dose fractionation and mask considerations," arXiv: 1804.03370 (2018).

[9] D. V. Strekalov, B. I. Erkmen, and N. Yu, "Ghost imaging of space objects," J. Phys. **414**, 012037 (2013).

[10] P. Clemente, V. Durán, V. Torres-Company, E. Tajahuerce, and J. Lancis, "Optical encryption based on computational ghost imaging," Opt. Lett. **35**, 2391–2393 (2010).

[11] F. Ferri, D. Magatti, L. A. Lugiato, and A. Gatti- "Differential Ghost Imaging". Phys. Rev. Lett. **104**, 253603 (2010).

[12] F. Ferri, D. Magatti, L. A. Lugiato, and A. Gatti. "Normalized ghost imaging". Phys. Rev. Lett. **104**, 253603 (2010).

[13] K. W. C. Chan, M. N. O'sullivan, and R. W. Boyd. "Optimization of thermal ghost imaging: high-order correlations vs. background subtraction". Opt. Express **18**,5562 (2010).

[14] L. Wang and S. Zhao, "Fast reconstructed and high-quality ghost imaging with fast Walsh-Hadamard transform," Photon. Res. **4**, 240–244 (2016).

[15] W.-K. Yu, M.-F. Li, X.-R. Yao, X.-F. Liu, L.-A. Wu, and G.-J. Zhai, "Adaptive compressive ghost imaging based on wavelet trees and sparse representation," Opt. Express **22**, 7133–7144 (2014).

[16] S. Jiao, "Design of optimal illumination patterns in single-pixel imaging using image dictionaries," arXiv: 1806.01340 (2018).

[17] Z. Zhang, M. Xiao, and J. Zhong, "Single-pixel imaging by means of Fourier spectrum acquisition," Nat. Commun. **6**, 6225 (2015).

[18] Z. Zhang, X. Wang, G. Zheng, and J. Zhong "Hadamard single-pixel imaging versus Fourier single-pixel imaging" Opt. Express **25**, 19619-19639 (2017)

[19] K. Shibuya1, K. Nakae1, Y. Mizutani, T. Iwata "Comparison of reconstructed images between ghost imaging and Hadamard transform imaging" Opt. Review **22**, 897–902 (2015)